

# HYBRID FILTER FOR REMOVING POWER-SUPPLY ARTIFACTS FROM EEG SIGNALS

Alina Santillán-Guzmán, Ulrich Heute  
Faculty of Engineering  
Christian-Albrechts-University of Kiel  
Kiel, Germany  
email: {asg, uh}@tf.uni-kiel.de

Ulrich Stephani, Hiltrud Muhle, and Andreas Galka  
Department of Neuropediatrics  
Christian-Albrechts-University of Kiel  
Kiel, Germany  
email: {stephani, muhle, a.galka}@pedneuro.uni-kiel.de

Michael Siniatchkin  
Department of Psychiatry, Psychosomatic Medicine and Psychotherapy  
Goethe-University  
Frankfurt am Main, Germany  
email: Michael.Siniatchkin@kgu.de

## ABSTRACT

Electroencephalographic (EEG) recordings are sometimes contaminated by spurious periodic components picked up from the power-supply equipment. The removal of these components presents a demanding problem because the current techniques do not suppress the artifact efficiently: Either the artifact is only partly eliminated, allowing some residual contribution in the desired signals, or not only the artifact is suppressed but also part of the valuable information. A hybrid filter, which employs both time-domain and frequency-domain representations of the data, is presented here to eliminate only the information considered as spurious. Through an application to real EEG data it is demonstrated that by removing the periodic components directly in time domain and by a subsequent phase and amplitude reconstruction in frequency domain, clean signals are obtained, even if the power of the spurious components is much larger than the power of the true signal. Unlike with most other approaches to filtering, special emphasis is put on optimal phase reconstruction.

## KEY WORDS

EEG, filtering, power-supply artifact.

## 1 Introduction

It is well known that electroencephalographic recordings (EEGs) may typically be disturbed by artifacts of physiological or technical origins that might obscure the brain activity. Among the physiological disturbances, eye movements are frequently found in the recordings. These artifacts typically consist of high-amplitude and low-frequency components, superimposed to the genuine signal. In the case of technical artifacts, a common example is the periodic AC potential of the power supply. In this case, most of the power of the EEG time series is concentrated in a (distorted) sine wave with a frequency of ca. 50 Hz, which is the frequency of the public AC power supply networks in many countries. The appearance of the data in time domain

may be dominated by this oscillation; in frequency domain sharp peaks at 50 Hz (or at the main line frequency) and its harmonics, which are rising above the broad-band spectrum of the actual EEG signal, are observed.

Different techniques have been used to suppress the power-line artifact. In [1] and in [2], adaptive filters have been employed for this purpose by using, as a reference, a simulated power-line signal. This signal was simulated using sinusoids with a frequency equal to that of the power supply (50 or 60 Hz). However, the power spectrum after filtering showed that the power-line artifact had been reduced but not totally suppressed. This might happen because the frequency of the simulated signal is not the true frequency of the power-supply (due to some instability of that frequency). Independent-Component Analysis (ICA) has also been used to suppress the power-line artifact. In [3], the extended infomax ICA was used to separate and remove this kind of artifact from the brain activity. The idea was to simulate the power-line and add it to the EEG data set, as if it was recorded simultaneously with the EEG signals. Then, by applying the extended infomax ICA, the power-line artifact was obtained in one of the components and was removed prior to the reconstruction of the signals. The power spectrum of the filtered data showed a reduction of the artifact, but not a complete suppression of it. This may occur because the removed component corresponded to the simulated signal (for being considered as a separate recorded signal), and not to the true artifact, which cannot be completely separated from the brain activity. For both, adaptive filters and ICA, an optimization of the amplitude, frequency and phase of the power-supply artifact is needed to obtain better results.

Either low-pass or notch filters with proper cutoff frequencies are also employed as a straightforward way to suppress this kind of artifacts. Low-pass filters are useful only when the content of the desired signal is below a certain cutoff frequency. All information beyond this frequency will be removed and in spite of the fact that such filters produce smooth and apparently clean data, it is not

obvious *a priori* which parts of the signal are considered as irrelevant.

A notch filter passes all frequencies except those in a narrow stop band around a center frequency. These filters will perform well if the frequency of the AC artifact is exactly at a known frequency (e.g. 50 Hz) and its multiples, and if the frequency is stable, which is not true for the case of biomedical signals [4]. An important parameter of the notch filters is the quality factor,  $Q$ , which is defined as the center frequency (i.e. the frequency to be removed) divided by the bandwidth. Although this method is quite fast and easy to implement, the  $Q$  factor should be wisely chosen to clean the signals properly; otherwise, the suppression of the artifact is not successful.

It is the purpose of this paper to show an approach that only removes those components which can convincingly be attributed to the spurious periodic signal and hence to reconstruct afterwards the full information of the original EEG signal without losing valuable information. Part of the work described in this paper is based on [5].

In Section II the filter design is explained, followed by a detailed description of the new algorithm in Section III. The application to real EEG data from a healthy subject is given in Section IV. Finally, Section V contains conclusions.

## 2 Filter Design

The filtering problem could be stated as a problem of *signal separation* [6], i.e. the following model is proposed

$$x(t) = s(t) + p(t) \quad (1)$$

where  $s(t)$  denotes the (unknown) true EEG signal and  $p(t)$  the (also unknown) pure spurious periodic component. Given only  $x(t)$ , the measured signal, an estimation of  $s(t)$  and  $p(t)$  for each time  $t$  is intended. However, this is impossible since there are infinitely many ways to decompose a number  $x$  into the sum of two other numbers  $s + p$ ; therefore, additional constraints are needed in order to obtain at least an approximate solution. The approach which will be presented in the following, will partly be based on time-domain, partly on frequency-domain representation; therefore, it is termed a hybrid filter.

### 2.1 Frequency-Domain Filtering

The frequency-domain equivalent of equation (1) is:

$$\tilde{x}(f) = \tilde{s}(f) + \tilde{p}(f) = a_s(f)e^{j\phi_s(f)} + a_p(f)e^{j\phi_p(f)} \quad (2)$$

where  $\tilde{x}(f)$ ,  $\tilde{s}(f)$ , and  $\tilde{p}(f)$  are the spectral representations of  $x(t)$ ,  $s(t)$ , and  $p(t)$ , respectively. This equation clearly shows the case of signal interference, i.e. the power spectrum of the superposition is not simply the sum of the power spectra of the components; rather, full complex numbers (with amplitudes  $a_s(f)$  and  $a_p(f)$ , and with

phases  $\phi_s(f)$  and  $\phi_p(f)$ ) are added, such that the relative phase differences have to be taken into account.

Since  $p(t)$  is a periodic signal,  $a_p(f)$  is zero for most frequencies (ignoring broadening effects for the moment), except for those where sharp lines are observed in the power spectrum of  $x(t)$ .

A pure frequency-domain filter can be implemented by removing the excess power in those frequency bins into which sharp lines are falling. The amplitudes of these bins can be corrected by averaging over an interval of neighbouring bins, provided these are not affected by broadening of the peak. By this approach, which is based on the assumption of smoothness of the true power spectrum, a reconstruction of the amplitudes  $a_s(f)$  can be approximated, but clearly not the phases  $\phi_s(f)$ . Full reconstruction of all  $a_s(f)$  and  $\phi_s(f)$  (and thereby also  $a_p(f)$  and  $\phi_p(f)$ ) is impossible, as already mentioned.

While this filter is already quite efficient for lines without broadening, it cannot directly be applied to very strong lines. The stronger peaks display a certain degree of spectral broadening or leakage, which is a result of windowing the time signal. The peaks at 50 Hz and the harmonics cover, through broadening, a few frequency bins, all of which would have to be corrected, if a pure frequency-domain filter was to be chosen.

### 2.2 Time-Domain Filtering

Since broadening is an intrinsic problem of the frequency domain, the removal of the spurious periodicities will be performed directly in time domain, i.e. an estimation of the true signal is obtained by

$$\hat{s}(t) = x(t) - \sum_n c_n \sin(2\pi f_n t + \varphi_n) \quad (3)$$

where  $n$  loops over all spurious peaks in the power spectrum of  $x(t)$ , and  $c_n$ ,  $f_n$ , and  $\varphi_n$  correspond to the amplitude, frequency, and phase of the  $n$ -th peak, respectively.

If correct values for the parameters  $c_n$ ,  $f_n$ , and  $\varphi_n$  are used, the sum should be able to exactly describe the spurious periodic component  $p(t)$  by expansion into its harmonics.

It is very important to obtain optimal estimates for the frequencies  $f_n$ ; it does not suffice to use those values corresponding to the DFT bins into which the sharp peaks are falling. Even tiny inaccuracies of the values  $f_n$  will cause a failure of the filtering. These have the effect that in the DFT the main peak is removed, but not all of the power which had leaked into neighbouring bins due to broadening is suppressed.

Therefore, optimal estimates for  $c_n$ ,  $f_n$ , and  $\varphi_n$  are necessary.

### 3 Algorithm Description

#### 3.1 Hybrid Filtering

First of all, segments of equal length are taken from the signal to be filtered, and the power spectrum is then computed per segment.

As already mentioned, in order for the time-domain filter to be successful, optimal estimates for  $c_n$ ,  $f_n$ , and  $\varphi_n$  are needed, which is not a trivial task, but approximations could be obtained by using an iterative parameter estimation.

In order to fit the parameters  $c_n$ ,  $f_n$ , and  $\varphi_n$  from equation (3) for each bin to be filtered, an objective function has to be minimized. Two choices are possible:

The first one consists of directly fitting the periodic disturbance to the time series:

$$F_1(c_n, f_n, \varphi_n) = \sum_t (x(t) - c_n \sin(2\pi f_n t + \varphi_n))^2 \quad (4)$$

The second choice is done by an indirect fitting such that as much power as possible is removed from the time series at the corresponding bin  $k$ :

$$F_2(c_n, f_n, \varphi_n) = |\tilde{\xi}(k)|^2, \quad (5)$$

where  $\tilde{\xi}(k)$  is the discrete Fourier transform of

$$\xi(t) = x(t) - c_n \sin(2\pi f_n t + \varphi_n). \quad (6)$$

This objective function itself is hybrid with respect to time and frequency domains.

For a practical implementation, it is advisable to define  $F_2(c_n, f_n, \varphi_n)$  not only as the power in bin  $k$ , but as the sum of the powers of a small interval around bin  $k$ , typically including a few neighbouring bins on each side.

The minimization itself is carried out by the Levenberg-Marquardt method with line search [7]. The initial values for the amplitudes are taken as the square-root of the power spectrum per segment. The frequencies are initialized to be multiples of the power supply frequency, and the phases are set to 0.

Using the objective function  $F_1$ , the minimization is performed for each bin to be filtered. This is achieved by removing each sine component as soon as its parameters have been estimated, and then estimating those of the next bin. In many cases this approach already yields quite convincing results, but in some cases, especially if several strong spurious lines are present, the parameter estimates are biased, especially the frequency estimates. Nevertheless, this approach is suitable for providing a good set of initial estimates.

An optimal parameter estimation can then be implemented by iteratively improving the estimates for all components. Given a set of estimates for all components  $c_{n,j}$ ,  $f_{n,j}$ ,  $\varphi_{n,j}$  (where  $n$  stands for the component, i.e. the bins to be filtered, and  $j$  counts the steps of the iteration), then

the preliminary filtered time series is formed by

$$\hat{s}_j(t) = x(t) - \sum_n c_{n,j} \sin(2\pi f_{n,j} t + \varphi_{n,j}). \quad (7)$$

For each bin to be filtered, i.e. each  $n$ , then a parameter estimation is repeated using the time series

$$x_{n,j}(t) = \hat{s}_j(t) + c_{n,j} \sin(2\pi f_{n,j} t + \varphi_{n,j}) \quad (8)$$

instead of  $x(t)$ , thereby removing all other lines as well as possible. This estimation step yields new improved estimates  $c_{n,(j+1)}$ ,  $f_{n,(j+1)}$ ,  $\varphi_{n,(j+1)}$ . The preliminary filtered time series  $\hat{s}_j(t)$  is not stored, but at each iteration the originally measured time series  $x(t)$  is used again, in order to create an improved filtered time series. Usually the iteration converges very fast, after two or three iterations no further improvements result. For this iterative approach the second objective function  $F_2$  is better suited.

As stated above, the parameter estimation is performed independently for each segment.

If all segments have the same length, and are taken from a longer time series without losing any data points in between, then for each spurious peak the phases of a series of consecutive segments must have constant phase differences between neighbouring segments. This property can be used to align the phase estimates of each segment.

#### 3.2 Phase Reconstruction

By the time-domain filtering as given by equation (3), the broadening problem is solved and, hence, also in frequency domain the true values  $a_s(f)$  and  $\phi_s(f)$  are retrieved for all bins, except for those into which the subtracted frequencies fall. In these bins the power should be zero after the filtering; but it is to be expected that also the true signal has some power in these bins. In order to restore this power, an average over an interval of neighbouring bins (after time-domain filtering it is certain that no broadening adds spurious power into these bins) is performed; the true phases, however, remain unknown.

Alternatively, equation (2) could be used in order to obtain an estimate of both  $a_s(f)$  and  $\phi_s(f)$  even for these bins. This again should be impossible, since the equation contains only two known quantities,  $a_x$  and  $\phi_x$ , but four unknowns,  $a_s$ ,  $a_p$ ,  $\phi_s$  and  $\phi_p$ . From the parameter estimation (as part of the time domain filtering) the values  $c_n$  and  $\varphi_n$  have been obtained, which, by assuming  $a_p \gg a_s$  (which is certainly true for strong lines), are considered as approximations for  $a_p$ ,  $\phi_p$ , and hence for  $\tilde{p}$ . Then by inverting the addition in the complex plane given by equation (2) into a complex subtraction, an estimation of  $\tilde{s}$ , i.e. of  $a_s$  and  $\phi_s$  is obtained. By obtaining an estimate for the phase  $\phi_s$ , an approximate phase reconstruction is now possible; also another amplitude estimate  $a_s$  results, which provides an alternative to the estimate obtained by averaging over neighbouring bins.

In the next section, the performance of the hybrid filtering is demonstrated by a real EEG example.

## 4 Application to Real Data

In order to demonstrate the performance of the hybrid filtering, real EEG data from a healthy subject are employed. These data have been recorded using a 64-EEG electrode system. The position and name of the electrodes have been standardized with the international 10-20 system. The sampling frequency is  $f_s = 1000$  Hz and the total length used here is 20000 sampling points, which corresponds to 20 s. The signal is decomposed into segments of 1000 points. The average power spectrum has been computed by squaring the absolute value of the Fourier transform of each segment and then averaging over the total number of segments.

Several EEG-electrode signals have been filtered successfully, but only the graphical results of one electrode is shown here as an example.

In Figure 1, a segment of the original time signal as well as the average power spectrum of the complete original signal are plotted. It is observed in Figure 1b that peaks at 50 Hz and its harmonics are present. They correspond to the power-supply artifact.

The hybrid filter is compared to a notch filter implemented in MATLAB by using the function *iircomb* [8], which gives the coefficients of an IIR filter according to the specified input arguments.

Three notch filters are implemented with different  $Q$  factors ( $Q = 10$ ,  $Q = 100$ , and  $Q = 200$ ). Each filter is applied to several EEG signals.

Figure 2 shows the average power spectra of the same signal as in Figure 1 before (dotted line) and after (continuous line) applying the notch filter with different  $Q$  values. If the quality factor is not chosen properly, either a loss (see Figure 2a) or an amplification (see Figure 2c) of the power at and around the center frequency could be obtained. Although there is a residual artifact at 250 Hz, the standard notch filter that produces the best result is that with a  $Q = 100$ , as can be graphically observed in Figure 2b.

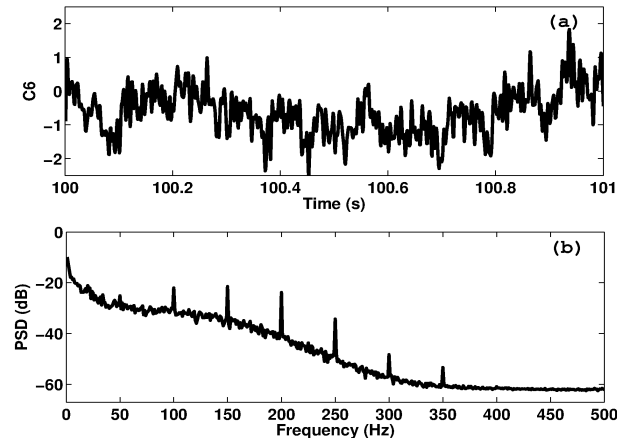


Figure 1: (a) One second out of twenty of the original time signal. (b) Average power spectrum of the complete signal.

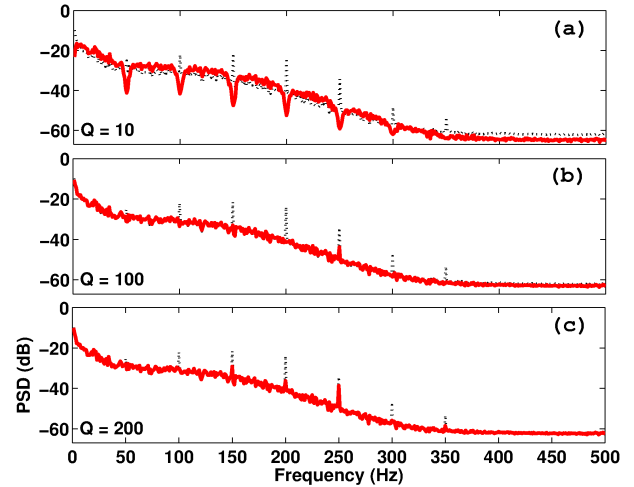


Figure 2: Notch Filters (continuous line) with different  $Q$  values: (a) with  $Q = 10$ , (b) with  $Q = 100$  and (c) with  $Q = 200$ . The dotted curves show the average power of the original signal. The best result is by using a  $Q = 100$ . With  $Q = 10$ , information at and around the center frequency is lost. With  $Q = 200$ , the artifact is not sufficiently suppressed.

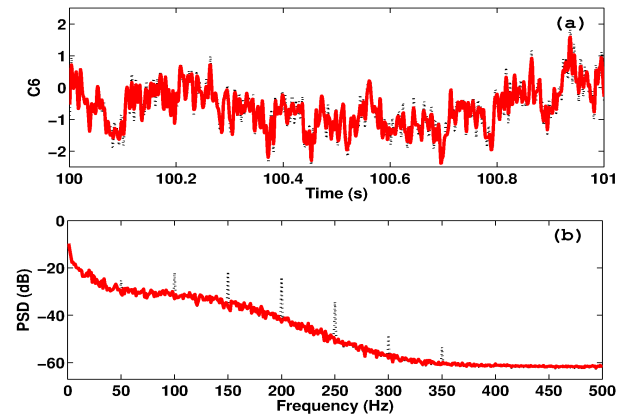


Figure 3: (a) One second out of twenty of the original (dotted line) and filtered (continuous line) time signals using the Hybrid Filter. (b) Original (dotted line) and filtered (continuous line) average power spectrum of the complete signal.

The hybrid filter is applied to the same set of 20 segments. The frequencies are initialized to be multiples of the power supply frequency, starting from 50 Hz and ending at 400 Hz. The result of applying the hybrid filter as described in section 3 is shown in Figure 3. In Figure 3a the original (dotted line) and the clean (continuous line) time signals are shown, and in Figure 3b the original (dotted line) and clean (continuous line) power spectra are plotted.

As can be seen in the figure, both in time domain and frequency domain, the filter has succeeded in removing the spurious periodic components, without removing any high-frequency power which has no relation to this particular artifact.

As mentioned above, the standard notch filter with

Table 1  
SNR comparison among the original signal ( $\text{SNR}_O$ ), standard notch filter ( $\text{SNR}_S$ ) and hybrid filter ( $\text{SNR}_H$ ).

Electrode	$\text{SNR}_O$ [dB]	$\text{SNR}_S$ [dB]	$\text{SNR}_H$ [dB]
C6	14.02	24.75	28.68
F3	19.74	25.32	28.19
FC4	16.32	24.22	28.91
CP3	14.82	24.26	29.67
P7	12.34	23.92	28.4

$Q = 100$  exhibits a similar behavior as the hybrid filter (see Figure 2b and Figure 3b). Taking this into account, this filter has been employed as a reference for comparison with the new approach.

To make an objective comparison, the Signal-to-Noise Ratio (SNR) has been computed. The SNR of the original signal (i.e. before filtering,  $\text{SNR}_O$ ), and the SNR after using the standard notch filter ( $\text{SNR}_S$ ) and after using the hybrid filter ( $\text{SNR}_H$ ) are shown in Table 1. This table shows the results for five electrodes, chosen randomly.

As can be seen in Table 1, the SNR increases after filtering. That suggests that both filters reduce the power-line artifact. However,  $\text{SNR}_H$  is larger than  $\text{SNR}_S$  at least by 3 dB and at most by 5.5 dB, i.e. the hybrid filter is better than the standard notch filter. In the case of the electrode C6, for example, the hybrid filter is about 4 dB better than the standard notch filter. When compared with  $\text{SNR}_O$ , the hybrid filter improves the signals at least by 8.5 dB and at most by 16 dB.

## 5 Conclusion

In this paper the problem of removing spurious peaks corresponding to the AC power supply in EEG data was treated. To solve that problem, the filtering task was interpreted as a signal-separation task, and a hybrid approach was designed to solve it, working partly in time domain and partly in frequency domain.

The periodic components are best removed from the data in time domain after fitting of the parameters of a decomposition into sine waves. Strong lines can be isolated very sharply in the frequency domain, despite considerable line broadening, and at neighbouring frequency bins the original spectrum, in terms of both amplitude and phase, can be retrieved very well.

Perfect signal separation from just one scalar time series is impossible. The power in those frequency bins into which the peak frequencies of the spurious lines fall cannot be separated exactly into spurious line power and power of the true signal within that bin; but it has been shown that through subtraction in the complex plane at least an approximate separation is possible. This is particularly interesting since it also enables a phase reconstruction.

According to the SNR, the standard notch filter and

the hybrid filter reduce the power-line artifact. However, it has been proven, graphically and objectively, that the hybrid filter is better than the standard notch filter implemented in MATLAB.

A disadvantage of this method, as compared to others, is the time-consuming optimization step. Depending on the clock frequency of the computer and the length of the signals to be filtered, the complete process might consume considerable time. However, it is the purpose of this method not to be fast but efficient, as it has been proven. Further research will focus on make it faster. Moreover, the filter described in this paper will be applied to different data sets, for example, to epilepsy data in order to test its performance.

## Acknowledgements

The authors would like to thank the German Research Foundation (Deutsche Forschungsgemeinschaft, DFG) who funded this research through the Collaborative Research Center SFB 855: "Biomagnetic Sensing".

## References

- [1] M. Golabbakhsh, M. Masoumzadeh, M. Farzan Sabahi, ECG and power line noise removal from respiratory EMG signal using adaptive filters, *Majlesi Journal of Electrical Engineering*, 5(4), 2011, 28-33.
- [2] A. Garcés Correa, E. Laciari, H. D. Patiño, M. E. Valentinuzzi, Artifact removal from EEG signals using adaptive filters in cascade, *Journal of Physics*, 90, 2007.
- [3] W. Zhou, J. Zhou, H. Zhao, L. Ju, Removing eye movement and power line artifacts from the EEG based on ICA, *Proc. 27th IEEE Conf. on Engineering in Medicine and Biology*, Shanghai, China, 2005, 6017-6020.
- [4] M. Ferdjallah, and R. E. Barr, Adaptive digital notch filter design on the unit circle for the removal of powerline noise from biomedical signals, *IEEE Transactions on biomedical engineering*, 41(6), 1994, 529-536.
- [5] A. Galka, U. Stephani, and H. Muhle, Hybrid nonlinear filtering approach to removing anharmonic periodic components from EEG time series, *ISM Research Memorandum*, 843, 2002.
- [6] J. F. Cardoso, Blind signal separation: Statistical principles, *Proc. IEEE*, 86, 1998, 2009-2025.
- [7] J. J. Mor, The Levenberg-Marquardt algorithm: Implementation and theory, in G. A. Watson (Ed.) *Numerical Analysis (Lecture Notes in Mathematics)*, 630 (Springer, 1977), 105-116.
- [8] The MathWorks, MATLAB R2010a.